American Mineralogist, Volume 93, pages 1581–1584, 2008

High-pressure study on lead fluorapatite

XI LIU, SEAN R. SHIEH,* MICHAEL E. FLEET, AND ARSLAN AKHMETOV

Department of Earth Sciences, University of Western Ontario, London, Ontario, N6A 5B7, Canada

ABSTRACT

The compressional behavior of a synthetic lead fluorapatite [$Pb_{9.35}(PO_4)_6F_2$] has been investigated in situ up to about 16.7 GPa at 300 K, using a diamond-anvil cell and synchrotron X-ray diffraction. We find that the compressibility of lead fluorapatite is significantly different from that of fluorapatite [$Ca_{10}(PO_4)_6F_2$], chlorapatite [$Ca_{10}(PO_4)_6Cl_2$], and hydroxylapatite [$Ca_{10}(PO_4)_6(OH)_2$]: lead fluorapatite is much more compressible, and elastically isotropic in the investigated pressure range. The pressure-volume data fitted to the third-order Birch-Murnaghan equation yield an isothermal bulk modulus (K_T) of 54.3(18) GPa and the pressure derivative (K'_T) of 8.1(6). If K'_T is fixed at 4, the obtained K_T is 68.4(16) GPa, which is approximately only two-thirds of the isothermal bulk modulus of the calcium apatites.

Keywords: Lead fluorapatite, compressibility, synchrotron X-ray diffraction, isothermal bulk modulus, high pressure

INTRODUCTION

Apatite group minerals have the general chemical formula $A_{10}(BO_4)_6X_2$, where A = Na^+, Ag^+, Ca^{2+}, Pb^{2+}, and rare-earth elements (REE^{3+}); B = P^{5+}, C^{3+}, S^{6+}, Si^{4+}, As^{5+}, and V^{5+}; and X = F^-, $(OH)^-$, Cl^-, $(CO_3)^{2-}$, $(HCO_3)^-$, O^{2-}, neutral molecules like H_2O, and vacancies (Pan and Fleet 2002). The mineralogy and geochemistry of the calcium phosphate apatites (hydroxylapatite, fluorapatite and francolite, and chlorapatite) have been extensively investigated because of their importance in igneous and metamorphic rocks, biomineralization and the environment, and agriculture (e.g., Ma et al. 1993; Pan and Fleet 2002; Hughes and Rakovan 2002; Fleet and Liu 2007a, 2007b). However, there are few studies of their thermodynamic properties, and our knowledge in this area is still very limited (Brunet et al. 1999; Comodi et al. 2001; Matsukage et al. 2004; Hovis et al. 2007).

In the present paper, we investigate the compressional behavior of a synthetic lead fluorapatite in situ in a diamond-anvil cell, using synchrotron X-ray diffraction. We are primarily interested in the effect of substitution by large cations at the Ca1 and Ca2 sites on the compressibility of apatites. The effect of substitution by F^-, Cl^-, and OH^- in the *c*-axis channel of calcium apatites has been studied by Brunet et al. (1999), and found to be very small (~5%). The effect of substitution at the B site has not been studied, but is likely to be small since the B site cation-anion polyhedra are rigid tetrahedra (e.g., Comodi et al. 2001).

EXPERIMENTAL METHOD

Lead fluorapatite was synthesized at 1 atm in a conventional muffle furnace. The starting material, a mechanical stoichiometric mixture of lead fluoride and lead orthophosphate, was encapsulated in a sealed platinum tube. The experimental temperature was set initially at 1373 K for 3 h (2° above the solidus of lead fluorapatite at 1 atm; Podsiadlo 1990), then decreased with a ramp of 1 K/min to 1273 K, and maintained at 1273 K for 10 h. The experimental capsule was then quickly quenched in a large volume of cold water.

The synthesis experiment produced large, transparent crystals of lead fluorapatite, along with a small amount of glass. The crystals were examined by optical microscopy, Fourier transform infrared spectroscopy (FTIR; Nicolet Nexus 670 FTIR spectrometer), powder X-ray diffraction (Rigaku D/MAX-B system; Co*K*α X-radiation), and electron probe microanalysis (EPMA; JEOL JXA-8600). In addition, one prismatic crystal was characterized by single-crystal X-ray structure study (Bruker-Nonius Kappa CCD diffractometer and graphite-monochromatized Mo*K*α X-radiation). The details of these various experimental techniques are well documented elsewhere (e.g., Fleet and Liu 2007b). Powder X-ray diffraction data confirmed that the crystalline phase was lead fluorapatite. The FTIR spectra suggested that these crystals were essentially OH-free, and the EPMA indicated that they were somewhat non-stoichiometric, with molar P/Pb = 0.642 ± 0.009. Preliminary refinement of the single-crystal X-ray data indicated two F anions per formula unit. Thus, the chemical formula of our lead fluorapatite is $Pb_{9.34}(PO_4)_6F_2$, with about 7 at% Pb assumed to be present as Pb^{4+}. Full characterization of this material is in progress and will be reported elsewhere.

The high-pressure angle dispersive X-ray diffraction experiments with a symmetrical diamond-anvil cell were carried out at beamline X17C, National Synchrotron Light Source, Brookhaven National Laboratory. A T301 stainless steel plate with an initial thickness of 250 μm was used as gasket. The central area of the plate was pre-indented to a thickness of about 40 μm, and a hole of 150 μm in diameter was drilled through it. Finely ground lead fluorapatite powders, plus a couple of ruby chips, were loaded with the pressure medium (a 4:1 methanol-ethanol mixture) into the hole in the gasket. The experimental pressure was determined by the ruby fluorescence method (Mao et al. 1978). The incident synchrotron radiation beam was monochromatized to a wavelength of 0.4066 Å, and its beam size was collimated to ~25 × 20 μm² in size. Two-dimensional images were recorded by a custom-built image plate. CeO_2 was used to calibrate the sample to detector distance as well as the orientation of the detector. The X-ray diffraction pattern was collected for five minutes at each pressure, and later integrated to give the conventional one-dimension profile using the Fit2D program (Hammersley 1996). Both GSAS refinement (Larson and Von Dreele 2000) and a weighted least-squares fit program were used to obtain the unit-cell parameters.

RESULTS AND DISCUSSION

At room temperature, lead fluorapatite was found to be stable up to at least 16.7 GPa (Fig. 1). The X-ray diffraction pattern at 16.7 GPa shows peak-broadening, which might imply the onset of lead fluorapatite instability; alternatively, the peak-broadening

---

* E-mail: sshieh@uwo.ca

0003-004X/08/0010–1581$05.00/DOI: 10.2138/am.2008.2816

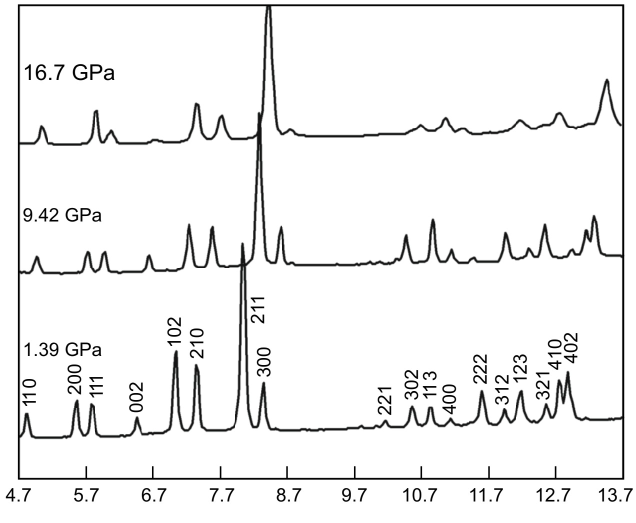

Figure 1. Examples of X-ray diffraction patterns of lead fluoraptite at 1.41, 9.39, and 16.7 GPa. Note the nominal peak-broadening at 16.7 GPa, which coalesces reflections 410 and 402.

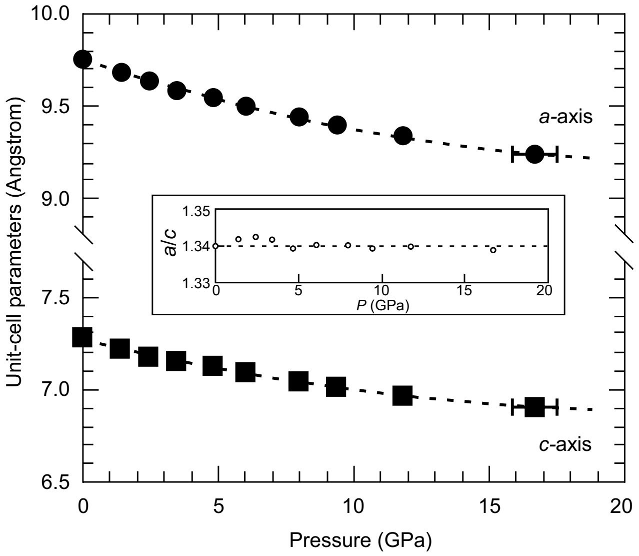

Figure 2. Pressure dependence of the unit-cell parameters *a* and *c* of lead fluorapatite at 300 K. The insert shows that the ratio of *a*/*c* for the studied *P* interval is essentially constant, indicating an isotropic elasticity for lead fluorapatite. Note that lengths of the error bars are generally equal to or smaller than the symbols.

might be due to the development of non-hydrostaticity of the pressure medium. The increased uncertainty in pressure at 16.7 GPa may be due to the bridging of the ruby chip to the diamonds (Table 1). Our pressure medium solidifies at ~10 GPa, however, the observed diffraction patterns at 16.7 GPa clearly indicate a typical lead fluorapatite structure (Table 1).

The room-pressure unit-cell parameters and volume of the studied lead fluorapatite are $a = 9.757(3)$ Å, $c = 7.283(4)$ Å, and $V = 600.4$ (3) Å^3; these values are comparable to the literature data for lead fluorapatite (e.g., $a = 9.75$ Å, $c = 7.30$ Å; Kreidler and Hummel 1970).

The effect of pressure on the unit-cell parameters and volume of lead fluorapatite is summarized in Table 1 and graphically shown in Figures 2 and 3. The pressure dependence of the *a* unit-cell parameter can be represented by the regression equation $a = 9.750(4) - 0.048(1)P + 0.0010(1)P^2$ and that of the *c* unit-cell parameter by $c = 7.270(6) - 0.035(2)P + 0.0007(1)$ P^2, with *a* and *c* in Å and *P* in GPa. The unit-cell parameters of lead fluorapatite have a non-linear dependence on pressure over this pressure range whereas those of calcium fluorapatite were reported to have a linear dependence on pressure (Comodi et al. 2001; Matsukage et al. 2004). The *a*/*c* ratio of lead fluorapatite over the investigated pressure range is essentially constant at 1.340(1), clearly indicating that lead fluorapatite is elastically isotropic (Table 1; Fig. 2). In contrast, previous studies of calcium fluorapatite revealed a weak compressional anisotropy (Sha et al. 1994; Brunet et al. 1999; Comodi et al. 2001; Matsukage et al. 2004).

The *P*-*V* data of lead fluorapatite are compared with the *P*-*V* data of calcium fluorapatite from Matsukage et al. (2004) in Figure 3. Clearly, lead fluorapatite is much more compressible than calcium fluorapatite. The non-linear pressure dependence of the unit-cell volume of lead fluorapatite is also obvious in Figure 3, the non-linearity being much more evident for the volume plot than for the unit-cell parameter plot of Figure 2. To determine the

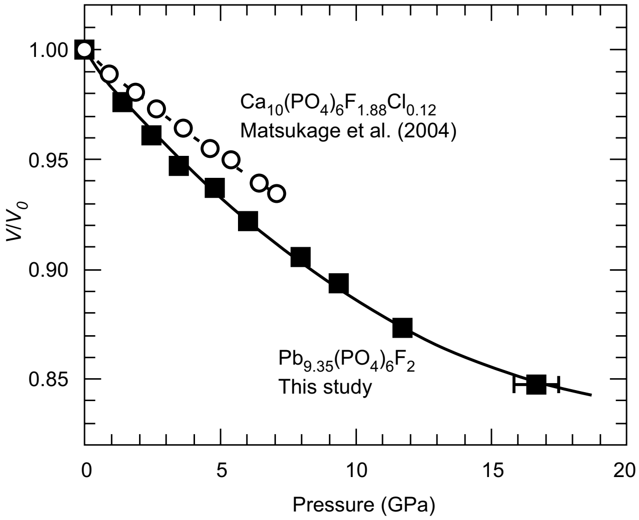

Figure 3. Pressure-volume data of lead fluorapatite at 300 K. Dashed and solid curves are data fitted to the third-order Birch-Murnaghan equation of state for lead fluorapatite and calcium fluorapatite. Note that the lengths of the error bars are generally equal to or smaller than the symbols.

Table 1. Unit-cell parameters of lead fluorapatite at different pressures

P (GPa)	*a* (Å)	*c* (Å)	*V* (Å^3)	*a*/*c*
0.0001	9.757(3)	7.283(4)	600.4(3)	1.340
1.39(2)	9.684(1)	7.218(2)	586.2(2)	1.342
2.44(2)	9.635(3)	7.179(4)	577.2(3)	1.342
3.45(2)	9.593(2)	7.151(2)	569.9(2)	1.341
4.71(10)	9.545(2)	7.129(4)	563.0(3)	1.340
6.05(3)	9.497(2)	7.088(4)	553.7(3)	1.340
7.96(2)	9.440(3)	7.045(5)	543.7(4)	1.340
9.42(3)	9.397(1)	7.017(2)	536.6(2)	1.339
11.8(2)	9.325(4)	6.961(6)	524.3(4)	1.340
16.7(8)	9.233(1)	6.897(1)	509.2(1)	1.339

Note: The number in parentheses represents one standard deviation in the right-most digit.

elastic parameters, the third-order Birch-Murnaghan equation of state (Birch 1947) was used:

$$P = 3K_T f_E (1 + 2f_E)^{\frac{5}{2}} [1 + \frac{3}{2}(K_T' - 4) f_E]$$

where P is the pressure, K_T the isothermal bulk modulus, K_T' the first pressure derivative of K_T, and f_E the Eulerian definition of finite strain, which is $[(V_0/V)^{2/3} - 1]/2$, respectively. In the Eulerian definition of finite strain, V_0 is the volume at zero pressure whereas V is the volume at high pressure. When K_T' is set as 4, the isothermal bulk modulus (K_T) of lead apatite is determined as 68.4(16) GPa, whereas the zero-pressure volume was determined as 598.1(8) Å^3. If K_T' is not fixed, the results of our best data-fitting are K_T = 54.3(18) GPa, K_T' = 8.1(6), and V_0 = 600.2(4) Å^3. By fixing K_T' to different values and calculating K_T, a correlation analysis of K_T and K_T' was also carried out and the result is shown in Figure 4. Compared to the isothermal bulk modulus of calcium fluorapatite (97.9 GPa from Brunet et al. 1999, 97.8 GPa from Comodi et al. 2001, and 91.5 GPa from Matsukage et al. 2004 when K_T' is fixed at 4), the isothermal bulk modulus of lead fluorapatite is substantially smaller (by about 30%). For the calcium phosphate apatites (hydroxylapatite, fluorapatite, and chlorapatite), and their mutual solid solutions, the variation of the isothermal bulk modulus is only about 5% (Brunet et al. 1999).

The differences in the elastic behavior of lead fluorapatite and calcium apatites are readily attributed to the different ionic size and bonding character of the large (A-site) cations, Pb^{2+} and Ca^{2+}: Pb^{2+} is a soft Lewis acid with a polarizability of 38.3 Å^3 and effective ionic radius (IR) for sixfold coordination of 1.19 Å, whereas Ca^{2+} is a hard Lewis acid with a polarizability of 5.2 Å^3 and IR of 1.00 Å (Pohl 1978; Shannon 1976). These major differences in chemical character are also reflected in the lower bulk moduli of β-PbO (31 GPa; Häussermann et al. 2001; van der Waal's bonded layer structure) and β-PbF$_2$ (61 GPa; Simmons and Wang 1971; fluorite structure) compared with CaO (112 GPa; Mammone et al. 1981; rocksalt structure) and CaF$_2$ (81 GPa; Angel 1993; fluorite structure), respectively. See also Badraoui et al. (2006) for discussion of the effect of the large cation interactions on the crystal chemistry of lead-strontium fluorapatite solid solutions.

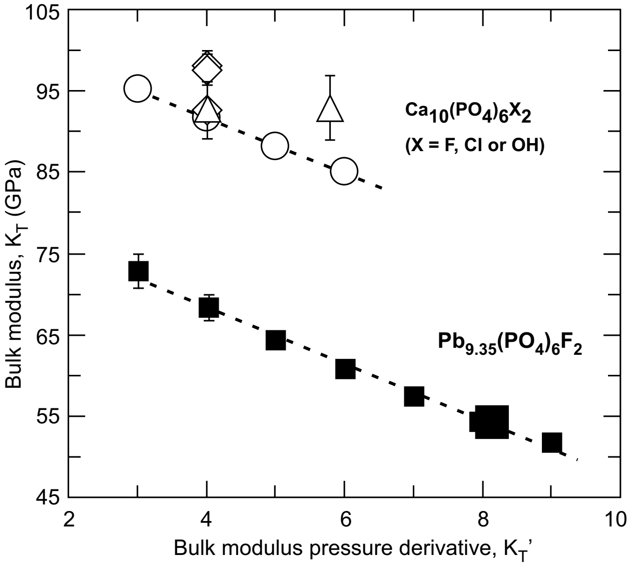

FIGURE 4. Comparison of the isothermal bulk moduli of lead fluorapatite with calcium hydroxylapatite-fluorapatite-chlorapatite at 300 K. Squares = lead fluorapatite (this study; the large filled square stands for our best data-fitting result); diamonds = calcium apatites (Brunet et al. 1999); triangles = calcium fluorapatite (Comodi et al. 2001); circles = calcium fluorapatite (Matsukage et al. 2004). Note that the lengths of the error bars are generally equal to or smaller than the symbols.

As in the calcium apatites, a series of hydroxyl-, fluor-, and chlor-substituted lead apatites, and their mutual solid solutions, also exist. These lead apatites have potentially important roles in the control of lead contamination of soil and immobilization of high-level radioactive waste (e.g., Ma et al. 1993; Kim et al. 2005). To date, most thermodynamic parameters of these phases are still not constrained. If the negligible effect of substitution among the channel anions on the bulk modulus of calcium apatites (Brunet et al. 1999) extends to the series of lead hydroxyl-fluor-chlorapatite, we would expect the bulk modulus of lead hydroxylapatite and lead chlorapatite to be very similar to that of lead fluorapatite.

ACKNOWLEDGMENTS

We thank J. Hu for her help with the synchrotron X-ray diffraction experiment. We thank two anonymous reviewers for their helpful comments that improved our paper. This work was financially supported by the Natural Sciences and Engineering Research Council of Canada.

REFERENCES CITED

Angel, R.J. (1993) The high-pressure, high-temperature equation of state of calcium fluoride, CaF$_2$. Journal of Physics: Condensed Matter, 5, 141–144.

Badraoui, B., Aissa, A., Bigi, A., Debbabi, M., and Gazzano, M. (2006) Structural investigations of lead-strontium fluoroapatites. Journal of Solid State Chemistry, 179, 3065–3072.

Birch, F. (1947) Finite elastic strain of cubic crystals. Physical Reviews, 71, 809–924.

Brunet, F., Allan, D.R., Redfern, S.A.T., Angel, R.J., Miletich, R., Reichmann, H.J., Sergent, J., and Hanfland, M. (1999) Compressibility and thermal expansivity of synthetic apatites, $Ca_5(PO_4)_3X$ with X = OH, F, and Cl. European Journal of Mineralogy, 11, 1023–1035.

Comodi, P., Liu, Y., Zanazzi, P.F., and Montagnoli, M. (2001) Structural and vibrational behaviour of fluorapatite with pressure. Part I: In situ single-crystal X-ray diffraction investigation. Physics and Chemistry of Minerals, 28, 219–224.

Fleet, M.E. and Liu, X. (2007a) Hydrogen-carbonate ion in synthetic high-pressure apatite. American Mineralogist, 92, 1764–1767.

——— (2007b) Coupled substitution of type A and B carbonate in sodium-bearing apatite. Biomaterials, 28, 916–926.

Hammersley, J. (1996) Fit2D report. Europe Synchrotron Radiation Facility, Grenoble, France.

Häussermann, U., Berastegui, P., Carlson, S., Haines, J., and Léger, J.-M. (2001) TlF and PbO under high-pressure: unexpected persistence of the stereochemically active electron pair. Angewandte Chemie, 113, 4760–4765.

Hovis, G., Harlov, D., Hahn, A., and Steigert, H. (2007) Enthalpies and volumes of F-Cl mixing in fluorapatite-chlorapatite crystalline solutions. Geophysical Research Abstracts, 9, 01748.

Hughes, J.M. and Rakovan, J. (2002) The crystal structure of apatite, $Ca_5(PO_4)_3$(F,OH,Cl). In M.J. Kohn, J. Rakovan, and J.M. Hughes, Eds., Phosphates, 48, p. 1–12. Reviews in Mineralogy and Geochemistry, Mineralogical Society of America, Chantilly, Virginia.

Kim, J.Y., Dong, Z., and White, T.J. (2005) Model apatite systems for the stabilization of toxic metals: II, Cation and metalloid substitutions in chlorapatites. Journal of American Ceramics Society, 88, 1253–1260.

Kreidler, E.R. and Hummel, F.A. (1970) The crystal chemistry of apatite: structure fields of fluor- and chlorapatite. American Mineralogist, 55, 170–184.

Larson, A.C. and Von Dreele, R.B. (2000) General Structure Analysis System (GSAS). Los Alamos National Laboratory Report LAUR 86-748.

Ma, Q.Y., Traina, S.J., Logan, T.J., and Ryan, J.A. (1993) In situ lead immobilization by apatite. Environmental Science and Technology, 27, 1803–1810.

Mammone, J.F., Mao, H.K., and Bell, P.M. (1981) Equations of state of CaO under static pressure conditions. Geophysical Research Letters, 8, 140–142.

Mao, H.K., Bell, P.M., Shaner, J.W., and Steinberg, D.J. (1978) Specific volume measurements of Cu, Mo, Pt, and Au and calibration of ruby R1 fluorescence pressure gauge for 0.006 to 1 Mbar. Journal of Applied Physics, 49, 3276–3283.

Matsukage, K.N., Ono, S., Kawamoto, T., and Kikegawa, T. (2004) The compressibility of a natural apatite. Physics and Chemistry of Minerals, 31, 580–584.

Pan, Y. and Fleet, M.E. (2002) Compositions of the apatite-group minerals: Substitution mechanisms and controlling factors. In M.J. Kohn, J. Rakovan, and J.M. Hughes, Eds., Phosphates, 48, p. 13–49. Reviews in Mineralogy and Geochemistry, Mineralogical Society of America, Chantilly, Virginia.

Podsiadlo, H. (1990) Polymorphic transitions in the binary system lead fluorapatite [$Pb_{10}(PO_4)_6F_2$]-calcium fluorapatite [$Ca_{10}(PO_4)_6F_2$]. Journal of Thermal Analysis, 36, 569–575.

Pohl, D. (1978) Electronic polarizabilities of ions in doubly refracting crystals. Acta Crystallographica, A34, 574–578.

Sha, M.C., Li, Z., and Bradt, R.C. (1994) Single-crystal elastic constants of fluorapatite, $Ca_5F(PO_4)_3$. Journal of Applied Physics, 75, 7784–7787.

Shannon, R.D. (1976) Revised effective ionic radii and systematic studies of interatomic distances in halides and chalcogenides. Acta Crystallographica, A32, 751–767.

Simmons, G. and Wang, H. (1971) Single Crystal Elastic Constants and Calculated Aggregate Properties: A Handbook. MIT Press, Cambridge, Massachusetts.

Manuscript received October 6, 2007
Manuscript accepted April 1, 2008
Manuscript handled by Przemyslaw Dera